PAPER

PLA-poloxamer/poloxamine copolymers for ligament tissue engineering: sound macromolecular design for degradable scaffolds and MSC differentiation†

Adrien Leroy,[a] Benjamin Nottelet,*[a] Claire Bony,[b] Coline Pinese,[a] Benoît Charlot,[c] Xavier Garric,[a] Danièle Noël*[b] and Jean Coudane[a]

The treatment of anterior cruciate ligament (ACL) failures remains a current clinical challenge. The present study aims at providing suitable degradable scaffolds for ligament tissue engineering. First, we focus on the design and the evaluation of poly(lactide)/poloxamer or poly(lactide)/poloxamine multiblock copolymers selected and developed to have suitable degradation and mechanical properties to match ACL repair. In the second part, it is shown that the copolymers can be processed in the form of microfibers and scaffolds consisting of a combination of twisted/braided fibers to further modulate the mechanical properties and prepare scaffold prototypes suitable for ligament application. Finally, after assessment of their cytocompatibility, the polymer scaffolds are associated with mesenchymal stem cells (MSCs). MSC differentiation toward a ligament fibroblast phenotype is promoted by a dual stimulation including an inductive culture medium and cyclic mechanical loads. RT-qPCR analyses confirm the potential of our scaffolds and MSCs for ACL regeneration with upregulation of some differentiation markers including Scleraxis, Tenascin-C and Tenomodulin.

1. Introduction

The anterior cruciate ligament (ACL) is known to have a poor healing capacity. A combination of various factors including low cellularity, low vascularity and the absence of blood clots at the site of injury to stabilize the two ligament ends and help tissue growth are often considered as the key mechanisms behind its failure to heal.[1] Therefore, after injury, these soft tissues are currently repaired using surgical procedures. Concerning ACL reconstruction, the risk of disease transmission, the lack of donors and the growing number of injuries requiring surgery (around 175 000 each year in the U.S.A) promoted the development of autograft techniques based on the use of hamstring or patellar tendons.[2] Despite the proven success of these autograft treatments, they are still facing limitations and

disadvantages like additional risks linked to the harvesting of the transplant, long recovery time (between 6 and 12 months), high surgery costs, limited availability of autologous tissues in the case of recurrent injuries and donor site morbidity which may induce residual pain, weakness and other complications.[2,3]

For all these reasons, the conception of alternative synthetic grafts has attracted growing attention in the last few decades. Following the detected failures of definitive synthetic grafts which were widely implanted in the 1980s and early 1990s,[4] advances in cell biology and in the field of biodegradable materials led researchers to develop ligament substitutes through tissue engineering. In particular, the strategy consisting of the association of a bioresorbable scaffold with cells in order to finally regenerate the tissues has been widely applied in the case of ACL tissue engineering. For the design of the scaffold, studies have been conducted on many kinds of materials including biological scaffolds (obtained from the dermis, the small intestine submucosa or the pericardium)[5] and natural polymers like silk,[6,7] collagen[8] and polysaccharides (chitosan, cellulose).[9,10] The main limitations of these materials come from the difficulty to finely control their mechanical and degradation properties. These properties are indeed extremely important since the scaffold needs to mimic the ligament's behavior to efficiently replace it. The scaffold has to

[a]*Institut des Biomolécules Max Mousseron (IBMM), UMR CNRS 5247, University of Montpellier 1, University of Montpellier 2, ENSCM, Faculty of Pharmacy, 15 Av. C. Flahault, F-34093 Montpellier, France.*
E-mail: benjamin.nottelet@univ-montp1.fr; Tel: +33 411 759 697
[b]*INSERM U844, Hôpital Saint-Eloi, 80 Av. Augustin Fliche, F-34295 Montpellier, France. E-mail: daniele.noel@inserm.fr*
[c]*Institut d'Electronique du Sud (IES), UMR CNRS 5412, University of Montpellier 2, Place E. Bataillon, F-34095 Montpellier Cedex 5, France*
†Electronic supplementary information (ESI) available. See DOI: 10.1039/c4bm00433g

take over the ligament during the regeneration without exhibiting very high initial mechanical properties that may induce a stress shielding phenomenon and ultimately lead to the formation of weak tissues. It should also be degradable to be fully replaced by neo-tissues at the end of the tissue repair process. To meet these requirements, attention has been paid to synthetic degradable polymers, especially to aliphatic polyesters like polylactide (PLA),[11–13] polyglycolide (PGA),[14] poly-(ε-caprolactone) (PCL),[10,12,15] and their copolymers.[7,16,17] Associating such polymers with textile processing allows one to obtain a wide range of properties and to modulate the mechanical properties to fit the ligament specific mechanical profile of ligaments (ESI Fig. S1†). However, it remains difficult to design a scaffold which meets the required specifications of degradation and mechanical properties. In this regard, many studies on ACL tissue engineering focus on the processing rather than on the materials chemistry. In contrast, our group being involved in the synthesis of original degradable aliphatic polyesters, especially of polylactide-polyethylene glycol (PLA-PEG) block copolymers for many years,[18] we were interested in the preparation of PLA copolymers showing high biocompatibility and were able to assess the ACL mechanical properties while featuring appropriate degradation rates for tissue engineering of ligaments. For this purpose, we recently synthesized PLA-poloxamer and PLA-poloxamine copolymers whose mechanical properties and degradation profiles may show promise for ligament tissue engineering.[19] It is to be noted that examples of PLA-poloxamers can be found in the literature. However, these polymers are designed for hydrogels and drug delivery applications, i.e. with macromolecular parameters (hydrophilicity, low molecular weight, and low to no crystallinity) far from those targeted for ligament repair.[20]

Finally, the last point to consider is that ligament tissue engineering not only requires good materials and sound scaffold architecture but also requires cellular proliferation and differentiation towards ligament forming cells. For this purpose, the use of mesenchymal stromal or stem cells (MSCs) as a cell source for the regeneration of ACL tissues is a common choice. In contrast to ACL fibroblasts, MSCs can easily be isolated from adult bone marrow or fat tissue and they exhibit high potential for proliferation and differentiation, which makes them particularly interesting as a suitable source for autologous transplant.[2,21,22] MSCs nevertheless require stimulation steps to differentiate toward a ligament fibroblast phenotype. Several strategies are currently used to induce this differentiation, including the use of growth factors.[2,22] For instance, epidermal growth factor (EGF), fibroblast growth factor (FGF), growth differentiation factor (GDF), insulin-like growth factor (IGF), platelet-derived growth factor (PDGF) or transforming growth factor-β (TGF-β) are known to induce cell proliferation, synthesis of extracellular matrix (ECM) proteins and, to some extent, orientation toward a fibroblastic phenotype.[23,24] However, despite a number of studies on this subject, there is still no standard procedure to specifically induce the differentiation toward ligament fibroblasts. Another popular strategy is the application of mechanical

stimulation to scaffolds seeded with MSCs, which will activate cell surface receptors and downstream intracellular signaling cascades to promote ECM production.[25] This technique gained popularity, thanks to the development of bioreactors designed to mimic the physiological conditions and to provide complex multidimensional strains (tension, torsion).[13,17,22,26]

The main objective of the present work is therefore to synthesize original degradable copolymers that will meet the demanding requirements of ligament tissue engineering scaffolds with respect to (i) mechanical properties, (ii) degradation rate and (iii) MSC differentiation. In the first part, original PLA/Pluronic and PLA/Tetronic copolymers are synthesized. Their properties and their processing to microfibers and structured scaffolds by twisting and braiding procedures are assessed. In the second part, MSCs' proliferation and differentiation on the obtained scaffolds are evaluated under dual stimulation with (i) inductive culture medium containing ascorbic acid and β-glycerophosphate that are known to promote cell proliferation, ECM production and differentiation,[27] and (ii) mechanical stimulation through cyclic loadings.

2.   Results and discussion

2.1.   Syntheses

In an attempt to provide an alternative to current degradable ligament tissue engineering scaffolds that have poor mechanical properties (natural polymers, amorphous PLA), or too low degradation rates (PCL, crystalline PLA), we synthesized multi-block copolymers made of PLA and Pluronic or Tetronic by ROP (Fig. 1). As described in our previous study, this strategy leads to a family of copolymers with good control of the macromolecular parameters (molecular weight, linear vs. star block copolymers, crystallinity). This control allows one to find the best match between the copolymer candidate and the application requirements. For example, such polymers have already been described in the literature, but to the best of our knowledge with oligoester segments, i.e. compositions and molecular parameters were chosen to meet the requirements of hydrogels and drug delivery applications.[20] In contrast, here we take advantage of the approach to meet mechanical and degradation properties suitable for ligament repair and to modulate and improve the biomaterial properties compared to the classically used PLA homopolymers.

Based on our past results, two copolymers were selected for ligament scaffold development as they showed good mechan-
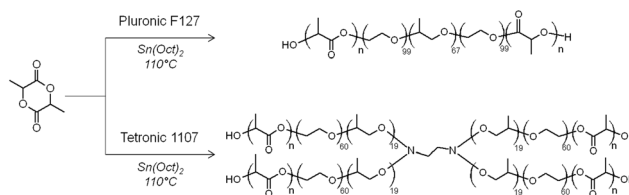

Fig. 1   General synthesis scheme of 94P200 and 94T200 copolymers.

Table 1 Mechanical properties of copolymers before processing and after processing compared to ACL mechanical properties (E = Young's modulus, σ_f = stress at failure, ε_f = strain at failure, σ_y = yield stress, ε_y = yield strain)

| Copolymer		E (MPa)	σ_y (MPa)	ε_y (%)	σ_f (MPa)	ε_f (%)
94P200	Film	556 ± 50	11 ± 1	2.8 ± 0.5	18 ± 2	613 ± 37
	Fiber	2181 ± 165	29 ± 3	1.3 ± 0.2	33 ± 1	11 ± 5
	Scaffold	346 ± 109	19 ± 3	6.4 ± 0.7	24 ± 3	78 ± 23
94T200	Film	455 ± 24	14 ± 1	3.5 ± 0.3	20 ± 1	765 ± 55
	Fiber	2299 ± 31	16 ± 1	0.7 ± 0.0	22 ± 6	10 ± 5
	Scaffold	440 ± 99	21 ± 2	5.4 ± 2.0	29 ± 1	20 ± 2
ACL[29]		49–163	—	7–16	14–36	19–36

ical and degradation properties in preliminary short term evaluations (7 weeks), while being highly compatible with L929 fibroblast culture.[19] More in detail, the targeted copolymers had a high molecular weight of 200 kg mol⁻¹ and were composed of crystalline PLA₉₄ side blocks (94% L-lactic units, 6% D-lactic units) associated with either Pluronic (94P200) or Tetronic (94T200) central blocks. Molecular weights of the copolymers were determined by ¹H NMR spectroscopy, using eqn (1) to (3), and were in good agreement with the targeted values. Molecular weights obtained from SEC analyses were *ca.* two times lower than those calculated from ¹H NMR spectra. This is in agreement with the literature where PLA analyses under the chosen SEC conditions classically give values about two times lower than theoretical ones.[28] Full details on the copolymer compositions and molecular weights are provided in ESI Table S1.†

Before scaffold processing, tensile tests were preliminarily carried out on copolymer films (Table 1). In this form, the mechanical properties were not those of native ACL but were still in the suitable range, which would allow a closer fit with ACL properties in the scaffold processing step. To further characterize the selected copolymers, their long term degradation behaviors *in vitro* were assessed on films in PBS (pH 7.4) at 37 °C and over a 6 month period. As shown in Fig. 2 the absence of degradation of the PLA₉₄ homopolymer (M_n = 200 000 g mol⁻¹) that may ultimately lead to weaker regener-

ated tissues was confirmed after six months with only 15% molecular weight loss. In contrast, the copolymers 94P200 and 94T200 with their hydrophilic central block showed a steady molecular weight decrease over the same period of time with *ca.* 30% after one month and 80% after six months. This intermediate degradation rate should be of advantage to avoid the well-known stress shielding effect compared to crystalline PLA homopolymers which are classically used despite a very slow degradation rate and high mechanical properties compared to ACL (ESI Fig. S2†).

2.2. Fiber properties

With the aim of developing scaffolds for ligament regeneration, both 94P200 and 94T200 copolymers were extruded to obtain microfibers. The average fiber diameter was calculated from the analysis of optical microscopy pictures with 5 fibers randomly selected from each picture. Fibers were obtained with average diameters of 162 ± 20 μm for the 94P200 copolymer and 193 ± 18 μm for the 94T200 copolymer. As degradable polymers like PLA are sensitive to thermal degradation, copolymer properties were characterized by SEC and DSC before and after extrusion. The results are summarized in Table 2. The placement in the extrusion chamber induced a significant degradation of the copolymers with *ca.* 40% molecular weight decrease and dispersity increasing from 2.0 to 2.5 for 94P200 and from 1.7 to 2.3 for 94T200. Despite the maintenance of copolymers under nitrogen flow during the process, these results indicated the beginning of thermal degradation by chain scission that has already been described in the literature.[30] Moreover, even though no significant change was observed in glass and melting temperatures, an important increase of the enthalpy of melting could be noticed for both 94P200 and 94T200 copolymers. This higher crystallinity can
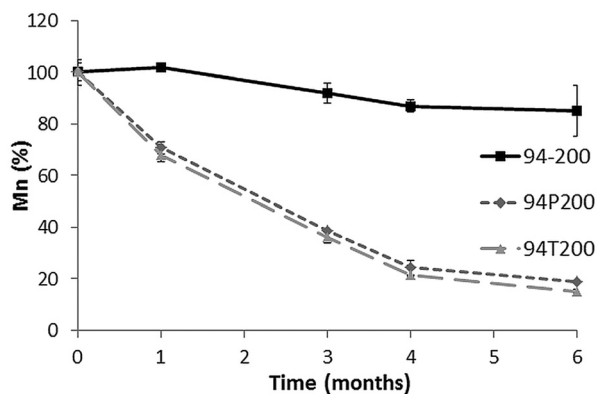
Fig. 2 Molecular weight evolution during *in vitro* degradation (PBS, pH 7.4, 37 °C) of 94P200 and 94T200 copolymers compared to the PLA homopolymer (94-200).

Table 2 Comparison of copolymer molecular weights and thermal properties before and after extrusion

Copolymer		$\bar{M}_n$ decrease	$Đ$	T_g (°C)	T_m (°C)	ΔH_m (J g⁻¹)
94P200	Before extrusion	42%	2.0	48	150	6.8
	After extrusion		2.5	46	152	14.4
94T200	Before extrusion	43%	1.7	46	150	3.6
	After extrusion		2.3	46	152	23.6

be explained both by the shortening of the polymer chains which promotes crystallization and by the chain stretching which occurs during the drawing step.

Tensile mechanical tests were carried out to evaluate the consequences of extrusion on mechanical properties. The results are summarized in Table 1 and compared with mechanical properties of copolymer films obtained by compression molding.[19] Extrusion caused major changes of the mechanical properties with strong increases of Young's moduli and characteristic stresses (E, σ_y and σ_f) whereas characteristic strains (ε_y and ε_f) strongly decreased after the process. These changes were expected as a result of the drawing step, which occasioned chain stretching during the extrusion process and led to more crystalline copolymers as shown by the increase of melting enthalpies (Table 2).

2.3. Scaffold mechanical properties

In the next step, and with the aim to yield mechanical properties closer to ACL, copolymer fibers were used to produce scaffolds (Fig. 3) following a twisting–braiding procedure reported to yield structures of interest for ligament repair.[31] Tensile mechanical tests were carried out on these scaffolds. A clear evolution of the scaffold mechanical profile was observed compared to that of fibers (Fig. 4a). While the fibers' stress–strain curve presented a linear region (elastic region governed by Hooke's law of elasticity) followed by a decrease in the slope (irreversible plastic deformation and damage region), the scaffold's stress–strain curve first showed a low-stress zone followed by linear and damaged regions. The twisting–braiding processing therefore leads to scaffolds with mechanical profiles similar to the typical three-stage ligament stress–strain curve (toe region, linear region and yield region).

This observation was confirmed by analysis of the mechanical properties obtained from these curves (Table 1). Compared to the fibers, scaffolds' Young's modulus (E) strongly decreased whereas the yield strain (ε_y) and strain at failure (ε_f) increased. By rendering microfibers the ability to slide along each other, the twisting–braiding processing induced these changes and allowed us to obtain properties closer to those of ACL. Interestingly, 94P200 and 94T200 copolymers had different behaviors concerning the yield stress (σ_y) and stress at failure (σ_f) after processing. Indeed, values significantly
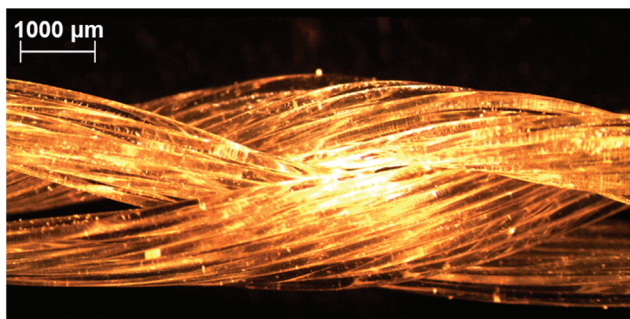

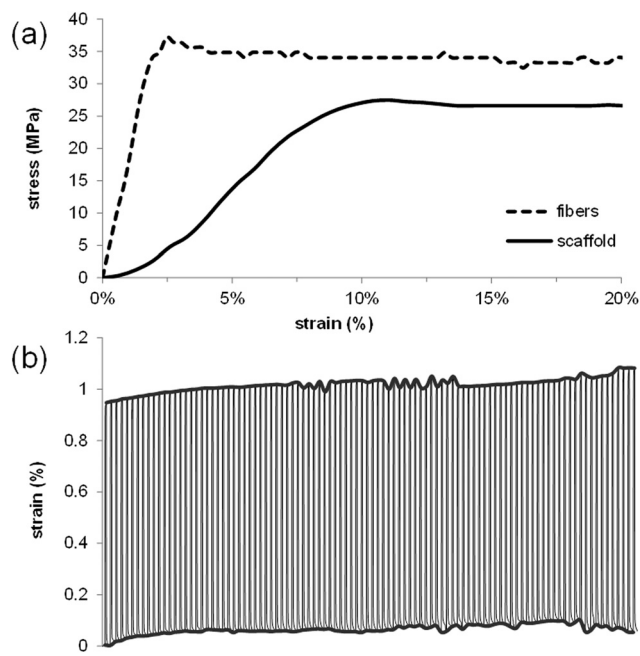Fig. 3 Optical microscopy picture of the ligament tissue engineering scaffold.

Fig. 4 Mechanical properties (a) typical stress–strain curves of extruded microfibers and twisted-braided scaffolds (b) evolution of the strain of a twisted-braided scaffold subjected to cyclic loads.

decreased for the linear 94P200 copolymer (from 29 to 19 MPa and from 33 to 24 MPa) whereas they slightly increased for the star 94T200 copolymer (from 16 to 21 MPa and from 22 to 29 MPa). Despite this difference, both types of scaffolds showed stresses at failure which were compatible with the ACL range of values (14–36 MPa).[29] On the other hand, Young's modulus, yield strain and strain at failure values measured on 94P200 scaffolds seemed more adaptable to the ACL requirements. Strain at failure values obtained with 94T200 scaffolds were low (20%) compared to 94P200 samples (78%) and ACL (19–36%). Finally, the yield strain value for the 94P200 scaffold (6%) was close to the lower range value for ACL (7%), and this characteristic may be further improved by tuning the scaffold shape in the future. All these observations led us to focus on 94P200 samples for the following experiments as properties were in agreement with those described by Laurencin *et al.* who developed scaffolds made from PLA fibers with architectures close to ours.[31] Their 4 braided 60–72 scaffold, which was considered as the best sample by the authors, exhibited a higher value of stress at failure (82 MPa) than our own scaffolds but the copolymerization of PLA and Pluronic allowed 94P200 scaffolds to reach higher values of Young's modulus and strain at failure (respectively 745 MPa and 31% for the 4 braided 60–72 sample). In addition, degradation being a key point for this approach, the possibility to modulate the degradation rate thanks to the copolymers[31] appears as an interesting alternative to pure crystalline PLA scaffolds.

Dynamic mechanical tests were finally performed to assess the ability of such twisted-braided scaffolds to withstand cyclic loadings. Scaffolds were subjected to 100 creep/recovery cycles

including a 1 MPa tensile stress phase (30 seconds) followed by a release of the applied load and a recovery period (90 seconds). Fig. 4b shows the evolution of the strain of a 94P200-based scaffold during these cycles and highlights the maximal and the residual strains. This test demonstrated that the scaffolds were able to bear such restrained loads at least a hundred times without breaking. Furthermore, it could be noticed that maximum and residual strains increased moderately through time. Maximal strain increased from 0.95% to 1.08% whereas residual strain was limited to 0.07%.

2.4. Cytocompatibility

Despite the proven cytocompatibility of PLA, Pluronic, Tetronic and their copolymers with L929 fibroblasts,[19,32] viability and proliferation of C3 MSCs were assessed on 94P200 and 94T200 twisted-braided scaffolds. First, proliferation of C3 MSCs seeded on scaffolds or in TCPS wells (positive control) was compared using the PrestoBlue assay during a 14-day period. As shown in Fig. 5, C3 MSCs highly proliferated during the overall period for all scaffolds. Starting from the 10th day, it can even be noticed that the fluorescence expressed with respect to the estimated available proliferation surface is statistically higher on copolymer scaffolds than on the TCPS positive control. This result not only demonstrated the excellent cytocompatibility of scaffolds made from 94P200 and 94T200 copolymers, but also suggested that the twisted-braided shape did not cause any significant loss of cell viability and enhanced cell proliferation.

Cell survival was also evaluated using the Live/Dead assay and confocal microscopy observations of scaffolds seeded with C3 MSCs. As shown in Fig. 6, after 10 days of culture, living C3 MSCs widely covered the surface of the scaffold. Moreover, almost no red staining was observed, confirming the absence of cytotoxic effects due to the copolymer. Living cells were also observed between the fibers inside the scaffold (ESI Movie S1†) indicating three-dimensional colonization of the twisted-braided structure. In conclusion, the data demonstrated adhesion and survival of cells, and high proliferation and 3D colonization by C3 MSCs, indicating the excellent cytocompat-
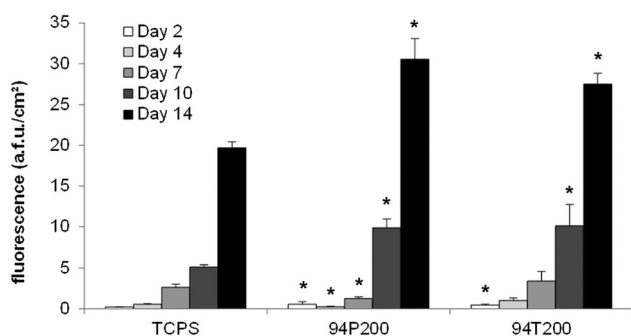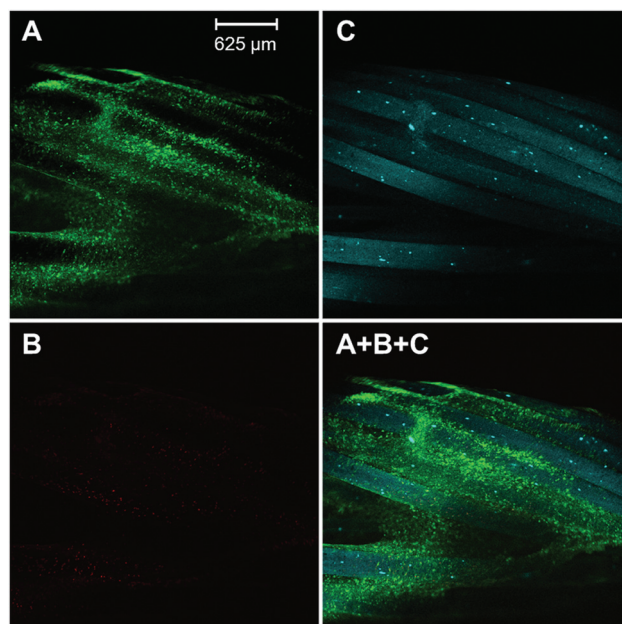

Fig. 6 Live/Dead assay fluorescence microscopy pictures after 10 days of proliferation of C3 cells on the 94P200 scaffold. Staining highlights viable cells in green (A), dead cells in red (B), copolymer autofluorescence in blue (C) and merge image (A+B+C).

ibility of the scaffolds and making them promising substrates for MSC proliferation and differentiation.

2.5. Differentiation assays with inductive medium

The first differentiation test was carried out on TCPS with C3 MSCs with three objectives: to assess the level of spontaneous differentiation in the absence of inductive medium, to assess the efficiency of the inductive medium containing ascorbic acid and β-glycerophosphate and to find the most suitable cell seeding density. The RT-qPCR analyses which were performed during the 21 days of culture revealed that the inductive effect of this culture medium is strongly dependent on the cell density. When cells were seeded at a high density (80 × 10^3 cells per well), most of the differentiation markers (Col I, Col III, Tnmd and Scx) were not modulated by the inductive medium (ESI Fig. S3†). Expression of Tnc even decreased after the 7th day and remained downregulated until the end of the experiment. On the other hand, significant upregulation of all the differentiation markers, except for Scx, was noticed on cells seeded at a lower density (16 × 10^3 cells per well) during the first 14 days. Interestingly, expression of Tnc and Tnmd was significantly upregulated at an earlier time point in inductive medium as compared to control conditions (peak at day 10 for Tnc and day 3 for Tnmd). No significant modulation of Scx was observed, although it seemed slightly increased at day 3 by the inductive medium with cells seeded at the lowest density. These results indicated that the selected inductive culture medium significantly upregulated the expression levels of most characteristic markers of the ligament fibroblast and therefore stimulated phenotypic orientation of C3 MSCs.

Fig. 5 *In vitro* proliferation of C3 cells on copolymer scaffolds. *Statistically significant difference in comparison with the TCPS control at the same time ($p < 0.05$).
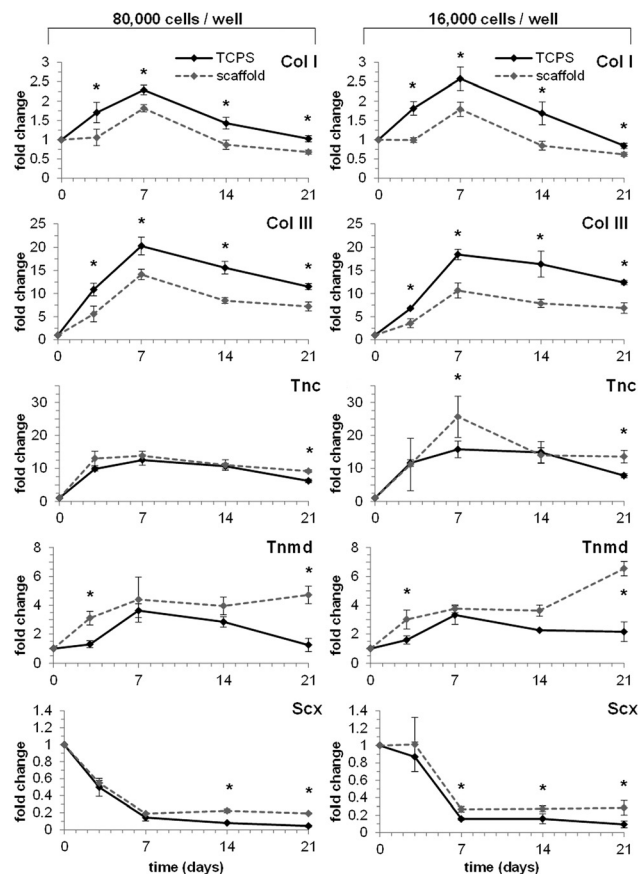
Fig. 7 Cell differentiation – expression of fibroblast-related markers by C3 cells maintained in inductive culture medium on TCPS or twisted-braided scaffolds *versus* time ($p < 0.05$).

Consequently, another experiment was performed to evaluate the influence of the culture substrate and confirm the importance of the seeding density in differentiation (Fig. 7). C3 MSCs were seeded at both densities (16×10^3 and 80×10^3 cells per well) on 94P200 scaffolds (chosen for their better mechanical properties) and TCPS wells and maintained in inductive medium. Whatever the seeding density, expression levels of Col I and Col III increased during the experiment but were significantly lower on scaffolds than on TCPS. In contrast, a significant increased expression of key ligamentocyte markers Tnc and Tnmd was observed at different time points during the assay when cells were seeded on scaffolds or on TCPS. The expression of the markers by cells seeded on scaffolds was however statistically higher on day 7 and 21 for Tnc and, day 3 and 21 for Tnmd. Although the expression of Scx decreased during the culture, it was higher on scaffolds than on TCPS during the experiment. Importantly with cells seeded on scaffolds, expression of the markers (in particular Tnc, Tnmd and Scx) remained stable or even increased by day 21 suggesting a sustained differentiation supportive effect of the scaffold. These results indicated that a low cell density favored differentiation of C3 MSCs when cultured in inductive medium suggesting the importance of the proliferation phase for better commitment toward the ligamentocyte lineage. All

the differentiation markers, with the exception of Scx, were increased when MSCs were cultured on scaffolds even though Col I and Col III were expressed at lower levels as compared to TCPS. Notably, the higher expression of Tnc, Tnmd and Scx, which are more specific for ligamentocytes, on scaffolds as compared to TCPS indicated that scaffolds were suitable for ligamentocyte differentiation.

2.6. Differentiation assays with inductive medium and mechanical stimulation

After having determined inductive conditions and in order to enhance ligamentocyte differentiation, we investigated the effect of a cyclic mechanical stimulation procedure applied to scaffolds. It was previously demonstrated that such stimulation processes may induce cellular responses including differentiation toward a ligamentocyte phenotype.[22,33] The behavior of cells cultured on these scaffolds under mechanical stimulation during 14 days was compared with that of cells cultured on scaffolds without any mechanical stimulation. As shown in Fig. 8, the mechanical stimulation did not improve the expression of Col I and led to a similar increase of Col III expression during the experiment to the one observed for non-stimulated cells. On the other hand, Tnc and Tnmd were significantly upregulated with expression peaks at the 7th day of culture while Scx was upregulated during the whole experiment. Importantly, we observed the increase of Scx expression compared to cells at the beginning of the test uniquely on cells cultured on scaffolds under stimulation (1.3 ± 0.2 fold increase at day 3 with respect to day 0 control). It should be noted that most of these results are in agreement with those presented by Subramony *et al.* in a similar study.[17] These authors also described a late upregulation of Col III, Tnc and Scx after 14 days of culture on aligned nanofibers of PLGA under mechanical stimulation in comparison with non-stimulated control samples.
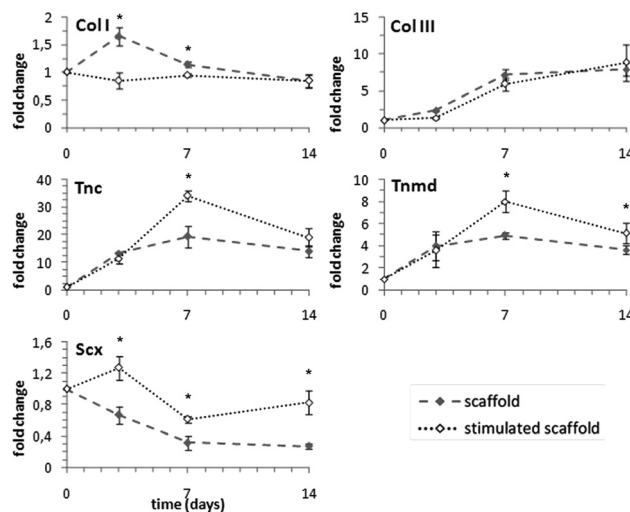

Fig. 8 Cell differentiation – expression of fibroblast-related markers by C3 cells maintained in inductive culture medium on scaffolds as a function of the mechanical stimulation *versus* time ($p < 0.05$).

In summary, although expression of Col I and Col III was not enhanced by the mechanical stimulation, that of other ligamentocyte markers did. Interestingly, mechanical stimulation induced a higher expression of Scx, an early transcription factor leading to the formation of ligament and tendon tissues,[34] and of Tnmd, a transmembrane protein and late marker of tendon and ligament formation regulated by Scx expression.[35] All these results suggested that the association of inductive medium and mechanical stimulation promoted the commitment of MSCs toward a ligament fibroblast phenotype. It is important to note that all the experiments were performed with murine mesenchymal stromal cells C3H10T1/2 that are currently used to evaluate the influence of scaffolds or molecules on cell differentiation.[36] Future work should confirm these promising results by assessing *in vitro* and *in vivo* long-term expression levels of markers from primary bone marrow-isolated mesenchymal stromal cells.

3. Conclusion

This work describes the development of prototype twisted-braided scaffolds for ligament tissue engineering based on original PLA-Pluronic or PLA-Tetronic architectures with intermediate degradation rates. These scaffolds obtained by twisting and braiding of copolymer microfibers exhibited mechanical properties close to those of a human ACL. They also proved to be able to withstand cyclic mechanical loadings and to have a high cytocompatibility with C3 MSCs. The Pluronic-based scaffolds were further shown to support MSC differentiation toward the ligament fibroblast phenotype when cells were cultured in inductive medium, with appropriate cell seeding density. Finally, scaffolds subjected to cyclic mechanical stimulation further stimulated the differentiation of MSCs. The increased expression levels of ligamentocyte lineage markers especially that of Scleraxis, a key marker of ligament and tendon differentiation, demonstrated the potential of the proposed scaffolds together with mechanical stimulation for future development of ligament tissue engineering.

4. Experimental section

4.1. Materials

Poloxamine (Tetronic® 1107; 15 000 g mol⁻¹) was purchased from BASF (Levallois Perret, France). Poloxamer (Pluronic® F-127; 12 600 g mol⁻¹), tin(ɪɪ) 2-ethylhexanoate (Sn(Oct)₂, 95%), dichloromethane (DCM), diethyl ether and tetrahydrofuran (THF) were purchased from Sigma-Aldrich (St-Quentin Fallavier, France), ʟ-lactide (ʟ-LA) and ᴅ,ʟ-lactide (ᴅʟ-LA) were purchased from Purac (Lyon, France). PrestoBlue™, Dulbecco's Modified Eagle Medium (DMEM) DMEM/F-12, Phosphate Buffered Saline (PBS), Dulbecco's Phosphate Buffered Saline (DBPS), Foetal Bovine Serum (FBS), penicillin, streptomycin, and glutamine were purchased from Invitrogen (Cergy Pontoise, France). BD Falcon™ Tissue Culture Polystyrene

(TCPS) multiwell plates were purchased from Becton Dickinson (Le Pont de Claix, France) and Corning® Costar® Ultra Low Attachment (ULA) multiwell plates were purchased from Sigma-Aldrich. All chemicals and solvents were used without purification.

4.2. Copolymer syntheses and degradation

PLA₉₄-Pluronic-PLA₉₄ and PLA₉₄-Tetronic-PLA₉₄ block copolymers (Fig. 1) were synthesized by ring-opening polymerization (ROP) following a procedure previously described by our group.[19] Typically, predetermined amounts of ʟ-LA, ᴅʟ-LA and Pluronic or Tetronic were introduced into a flask and Sn(Oct)₂ (0.1 molar% with respect to LA units) was then added. After degassing, the flask was sealed under vacuum and polymerization was allowed to proceed at 110 °C. After 5 days, the copolymer was recovered by dissolution in DCM and precipitation in cold diethyl ether. Finally, the product was dried under reduced pressure to constant mass. The copolymers were obtained with an average yield of 81% (40.5 g).

¹H NMR: (300 MHz; CDCl₃): δ (ppm) = 5.1 (q, 1H, CO–CH-(CH₃)–O), 3.6 (s, 4H, CH_2–CH₂–O), 3.5 (m, 2H, CH(CH₃)–CH_2–O), 3.4 (m, 1H, CH(CH₃)–CH₂–O), 1.5 (m, 3H, CO–CH(CH_3)–O), 1.1 (m, 3H, CH(CH_3)–CH₂–O).

The polymerization degree of PLA blocks and the molecular weight of the synthesized block copolymers were calculated using the following equations.

$$DP_{PLA} = DP_{PEO}/(EO/LA) \tag{1}$$

For PLA-Pluronic-PLA copolymers:

$$M_n = 2 \times (DP_{PLA} \times 72) + M_{n\ Pluronic} \tag{2}$$

For PLA-Tetronic-PLA copolymers:

$$M_n = 4 \times (DP_{PLA} \times 72) + M_{n\ Tetronic} \tag{3}$$

EO/LA being the ratio of ethylene oxide and lactyl units and PO/LA being the ratio of propylene oxide and lactyl units calculated from ¹H NMR spectra.

For tensile tests and degradation tests on films, sample plates were prepared by compression of the polymer in a stainless steel mould for 10 min at 200 °C and 8 tons using a Carver press (4120).

For degradation test samples were cut (30 × 10 × 0.5 mm) and were then placed in 8 mL of PBS (pH 7.4) at a constant temperature (37 °C) under stirring. At scheduled time points, samples were removed from PBS, and dried to constant mass before SEC analysis for molecular weight determination.

4.3. Scaffold design

Micro-fibers were obtained by processing the copolymers with DSM Xplore equipment combining a micro-compounder and a micro-fiber spin device kindly made available by Pr Sophie Duquesne from the Ecole Nationale Supérieure de Chimie de Lille (ENSCL) and the Unité Matériaux et Transformations (UMET – UMR CNRS 8207). In order to obtain microfibers, 20 g of PLA-Pluronic or PLA-Tetronic copolymer were intro-

duced in a DSM Xplore twin-screw micro-compounder equipped with an extrusion chamber of 15 mL and co-rotating twin-screws maintained under a nitrogen flow. First, the temperature of the extrusion chamber was set at 200 °C and the screw speed was set at 80 rpm for around 5 minutes. The extrusion was then realized at a screw speed of 15 rpm through a 1 mm diameter spinneret and the monofilament was drawn and collected using a DSM Xplore Fiber Spin Line equipped with a drawing roll and a collecting roll (spinning velocity of 30 m min^{-1}).

The extruded micro-fibers were used to make fibrous scaffolds by a method combining twisting and braiding processes. To prepare one scaffold, 30 micro-fibers were first cut in long segments (75 cm) and separated into 3 groups. Each group of 10 micro-fibers was twisted for 10 seconds in a clockwise direction using a rotary engine. The 3 bundles were then braided together to form the scaffold (Fig. 3).

4.4. Characterization

The number average molecular weight (M_n) and dispersity ($Đ$) of the polymers were determined by size exclusion chromatography (SEC) using a Viscotek GPCMax autosampler system fitted with two Viscotek LT5000L mixed medium columns (300 × 7.8 mm), and a Viscotek VE 3580 RI detector. The mobile phase used was THF at 1 mL min^{-1} flow and 30 °C. Typically, the polymer (20 mg) was dissolved in THF (2 mL) and the resulting solution was filtered through a 0.45 μm Millipore filter before injection of 20 μL of the filtered solution. M_n and $Đ$ were expressed according to calibration using polystyrene standards.

^{1}H NMR spectra were recorded at room temperature using an AMX300 Bruker spectrometer operating at 300 MHz. Deuterated chloroform was used as the solvent, chemical shifts were expressed in ppm with respect to tetramethylsilane (TMS).

Differential scanning calorimetry (DSC) measurements were carried out under nitrogen on a Perkin Elmer Instrument DSC 6000 thermal analyzer. Samples were subjected to the first heating scan to 200 °C followed by cooling (10 °C min^{-1} from 200 °C to 100 °C, and 5 °C min^{-1} from 100 °C to −30 °C) and the second heating scan to 200 °C (10 °C min^{-1}). The glass transition temperature (T_g), melting temperature (T_m) and melting enthalpy (ΔH_m) were measured on the second heating ramp.

Tensile mechanical tests were performed on scaffold samples and on groups of 10 parallel isolated micro-fibers. The samples (30 mm) were analyzed at 37 °C in an Instron 4444 at a crosshead speed rate of 5 mm min^{-1}, each sample being loaded to failure. The samples were analyzed in triplicate and Young's modulus (E, MPa), stress at failure (σ_f, MPa), strain at failure (ε_f, %), yield stress (σ_y, MPa), and yield strain (ε_y, %) were expressed as the mean value of the three measurements. E was calculated using the second linear portion of the stress–strain curves corresponding to ACL's linear region (ESI Fig. S1†).

Dynamic tensile mechanical tests were also performed on scaffolds to study their resistance to cyclic mechanical loading. The samples (10 mm) were analyzed at 37 °C in a Perkin Elmer Instrument DMA 7 mechanical analyzer. The samples were subjected to 100 creep/recovery cycles (1 MPa tensile stress during 30 seconds followed by a release of the applied load and a recovery period of 90 seconds).

4.5. Cell culture

Murine mesenchymal stromal cells C3H10T1/2 (designated C3 MSCs thereafter) were used to assess the *in vitro* cytocompatibility of the scaffolds and to carry out the differentiation tests. Cells were cultured in a 5% CO$_2$ incubator at 37 °C in proliferative medium composed of DMEM with phenol red (+PR) or DMEM/F-12 without phenol red (−PR) supplemented with 10% FBS, penicillin (100 U mL^{-1}), streptomycin (100 μg mL^{-1}) and glutamine (2 mM). All scaffold samples used in these studies were disinfected in ethanol for 30 min before immersion in a solution of sterile PBS containing penicillin and streptomycin (1 mg mL^{-1}) and incubation for 48 h at 37 °C. The samples were then rinsed 2 times with sterile PBS before soaking for 12 h in sterile PBS.

4.6. Cytocompatibility

To evaluate the proliferation potential of C3 cells, samples (10 mm long) were cut from scaffolds and placed in ULA 6-well plates to avoid cells growing on the bottom of the wells. Samples and empty TCPS 6-well plates were seeded with 10^4 C3 cells which were then maintained in proliferative medium (−PR). Viability and proliferation were evaluated after 2, 4, 7, 10 and 14 days using the PrestoBlue assay, a cell-permeable resazurin-based viability reagent which reflects the number of living cells present at a given time point. At scheduled time points, proliferative medium was removed and replaced by 5 mL of fresh medium containing 10% of PrestoBlue. After 30 minutes of incubation at 37 °C, 200 μL of the supernatant were taken and analyzed for fluorescence (excitation 560 nm, emission 590 nm) with a Varioskan Flash Multimode microplate reader (Thermo Scientific, Waltham, USA). The results were divided by the estimated surface available for cell proliferation (9.4 cm^2 for TCPS wells, 1.5 cm^2 for 94P200 scaffolds and 1.8 cm^2 for 94T200 scaffolds) and expressed as arbitrary fluorescence units (a.f.u. cm^{-2}).

Cell adhesion and viability were assessed using the Promo-Kine Live/Dead cell staining kit (PromoCell GmbH, Heidelberg, Germany). After culturing in proliferative medium (+PR), 4 × 10^5 cells were seeded on disinfected scaffold samples (15 mm) placed in ULA 24-well plates. After 10 days, proliferative medium was removed and samples were rinsed 3 times with sterile PBS to eliminate non-adherent cells. C3 cells were then incubated in the presence of a Live/Dead staining solution (2 μM Calcein-AM and 4 μM Ethidium homodimer III) at 37 °C for 15 min and then fixed with 4% paraformaldehyde for 10 min. Cells were observed under a Leica Microsystems Macroconfocal LSI microscope (Leica Microsystems GmbH, Wetzlar, Germany).

4.7. Differentiation tests

Differentiation of C3 MSCs was induced after seeding at different densities (16×10^3 and 80×10^3 C3 cells) on TCPS and culture in inductive medium composed of proliferative medium (+PR) supplemented with ascorbic acid (50 μg mL^{-1}) and β-glycerophosphate (10 mM) or in proliferative medium (+PR) (negative control). At scheduled time points (3, 7, 10, 14 and 21 days), cells were trypsinized and recovered for RNA analysis by RT-qPCR.

To study the influence of the culture substrate on the cells, 16×10^3 C3 MSCs were seeded in empty TCPS 24-well plates or on disinfected scaffold samples (15 mm). Cells were maintained in inductive medium for 3, 7, 10, 14 and 21 days. At scheduled time points, cells were trypsinized and recovered for RNA analysis by RT-qPCR.

For mechanical stimulation, samples (55 mm) were cut from scaffolds and used to obtain loops by welding their ends together. After disinfection, these loops were placed in ULA 6-well plates, seeded with 58×10^3 C3 cells which were then maintained in proliferative medium (+PR). After 2 days (day 0), proliferative medium was replaced by inductive medium and seeded loops were maintained under static conditions (negative control) or dynamic mechanical conditions. The mechanical stimulation process consisted of a 5% cyclic strain applied at 0.5 Hz for 1 hour every 1 or 2 days. Cyclic strains were applied to culture medium using an N-381 NEXACT® piezoelectric motor (Physik Instrumente GmbH & Co, Karlsruhe, Germany) able to generate up to 10 N force (ESI Fig. S4†). After 3 (3 sessions of stimulation), 7 (4 sessions) and 14 days (7 sessions), cells were trypsinized for RNA analysis by RT-qPCR.

4.8. Total RNA extraction and RT-qPCR

C3 cells were washed with PBS and mechanically dissociated in lysis buffer for total RNA extraction using the RNeasy Mini Kit and a QIAcube automated station according to the manufacturer's instructions (Qiagen S.A., Courtabœuf, France). RNA (0.5 to 1 μg) was reverse transcribed using the M-MLV enzyme (Life technologies, Saint-Aubin, France). Primers were designed using Primer3 software (ESI Table S2†) and purchased from MWG (Eurofins genomics, Courtabœuf, France). PCR was carried out on 20 ng of cDNA samples using 5 μmol L^{-1} of each primer. Real-time PCR was performed using the SYBR Green I Master Kit and a LightCycler® 480 detection system, following the manufacturer's recommendations and analysis of the mRNA expression level was performed using the dedicated software (Roche Applied Science, Meylan, France). The expression level of transcripts was normalized to the glyceraldehyde-3-phosphate dehydrogenase (GAPDH) housekeeping gene and expressed as a fold change according to the formula $2^{-\Delta\Delta Ct}$.

4.9. Statistical analyses

The results corresponded to separate experiments conducted in triplicate and values are given as mean ± SD. Statistical analyses were performed with the GraphPad Prism software (San Diego, CA). A comparison between several groups was performed using a non-parametric Mann–Whitney test (a level of $p < 0.05$ was considered statistically significant).

References

1 (a) V. B. Duthon, C. Barea, S. Abrassart, J. H. Fasel, D. Fritschy and J. Ménétrey, *Knee Surg. Sports Traumatol. Arthrosc.*, 2006, **14**, 204; (b) T. Zantop, W. Petersen, J. Sekiya, V. Musahl and F. Fu, *Knee Surg. Sports Traumatol. Arthrosc.*, 2006, **14**, 982; (c) M. M. Murray and B. C. Fleming, *J. Orthop. Res.*, 2013, **31**, 1501.

2 N. L. Leong, F. A. Petrigliano and D. R. McAllister, *J. Biomed. Mater. Res., Part A*, 2013, **102**, 1614.

3 J. Cournapeau, S. Klouche and P. Hardy, *Orthop. Traumatol. Surg. Res.*, 2013, **99**, 196.

4 (a) C. Legnani, A. Ventura, C. Terzaghi, E. Borgo and W. Albisetti, *Int. Orthop.*, 2010, **34**, 465; (b) A. Ventura, C. Terzaghi, C. Legnani, E. Borgo and W. Albisetti, *Knee*, 2010, **17**, 108.

5 (a) X. Chen, Y.-Y. Qi, L.-L. Wang, Z. Yin, G.-L. Yin, X.-H. Zou and H.-W. Ouyang, *Biomaterials*, 2008, **29**, 3683; (b) E. T. Ricchetti, A. Aurora, J. P. Iannotti and K. A. Derwin, *J. Shoulder Elbow Surg.*, 2012, **21**, 251.

6 (a) S. Farè, P. Torricelli, G. Giavaresi, S. Bertoldi, A. Alessandrino, T. Villa, M. Fini, M. C. Tanzi and G. Freddi, *Mater. Sci. Eng., C*, 2013, **33**, 3601; (b) A. L. Oliveira, L. Sun, H. J. Kim, X. Hu, W. Rice, J. Kluge, R. L. Reis and D. L. Kaplan, *Acta Biomater.*, 2012, **8**, 1530.

7 C. Vaquette, C. Kahn, C. Frochot, C. Nouvel, J.-L. Six, N. D. Isla, L.-H. Luo, J. Cooper-White, R. Rahouadj and X. Wang, *J. Biomed. Mater. Res., Part A*, 2010, **94**, 1270.

8 (a) E. Gentleman, G. Livesay, K. Dee and E. Nauman, *Ann. Biomed. Eng.*, 2006, **34**, 726; (b) S. J. Kew, J. H. Gwynne, D. Enea, M. Abu-Rub, A. Pandit, D. Zeugolis, R. A. Brooks, N. Rushton, S. M. Best and R. E. Cameron, *Acta Biomater.*, 2011, **7**, 3237.

9 (a) T. Irie, T. Majima, N. Sawaguchi, T. Funakoshi, S.-I. Nishimura and A. Minami, *J. Biomed. Mater. Res., Part*

A, 2011, **97**, 111; (*b*) A. P. Mathew, K. Oksman, D. e. Pierron and M.-F. o. Harmand, *Carbohydr. Polym.*, 2012, **87**, 2291.

10 H.-J. Shao, C. S. Chen, Y.-T. Lee, J.-H. Wang and T.-H. Young, *J. Biomed. Mater. Res., Part A*, 2010, **93**, 1297.

11 (*a*) J. G. Barber, A. M. Handorf, T. J. Allee and W.-J. Li, *Tissue Eng., Part A*, 2013, **19**, 1265; (*b*) J. W. Freeman, M. D. Woods, D. A. Cromer, E. C. Ekwueme, T. Andric, E. A. Atiemo, C. H. Bijoux and C. T. Laurencin, *J. Biomech.*, 2011, **44**, 694; (*c*) N. Tovar, S. Bourke, M. Jaffe, N. S. Murthy, J. Kohn, C. Gatt and M. G. Dunn, *J. Biomed. Mater. Res., Part A*, 2009, **93**, 738.

12 M. R. Ladd, S. J. Lee, J. D. Stitzel, A. Atala and J. J. Yoo, *Biomaterials*, 2011, **32**, 1549.

13 D. C. Surrao, J. C. Y. Fan, S. D. Waldman and B. G. Amsden, *Acta Biomater.*, 2012, **8**, 3704.

14 H. H. Lu, J. A. Cooper, S. Manuel, J. W. Freeman, M. A. Attawia, F. K. Ko and C. T. Laurencin, *Biomaterials*, 2005, **26**, 4805.

15 H.-J. Shao, Y.-T. Lee, C.-S. Chen, J.-H. Wang and T.-H. Young, *Biomaterials*, 2010, **31**, 4695.

16 (*a*) C. Laurent, D. Durville, D. Mainard, J.-F. Ganghoffer and R. Rahouadj, *J. Mech. Behav. Biomed.*, 2012, **12**, 184; (*b*) J. Lee, W. I. Choi, G. Tae, Y. H. Kim, S. S. Kang, S. E. Kim, S.-H. Kim, Y. Jung and S. H. Kim, *Acta Biomater.*, 2010, **7**, 244.

17 S. D. Subramony, B. R. Dargis, M. Castillo, E. U. Azeloglu, M. S. Tracey, A. Su and H. H. Lu, *Biomaterials*, 2013, **34**, 1942.

18 (*a*) I. Rashkov, N. Manolova, S. M. Li, J. L. Espartero and M. Vert, *Macromolecules*, 1996, **29**, 50; (*b*) A. Harrane, A. Leroy, H. Nouailhas, X. Garric, J. Coudane and B. Nottelet, *Biomed. Mater.*, 2011, **6**, 065006.

19 A. Leroy, C. Pinese, C. Bony, X. Garric, D. Noël, B. Nottelet and J. Coudane, *Mater. Sci. Eng., C*, 2013, **33**, 4133.

20 (*a*) W. Zhu, B. Wang, Y. Zhang and J. Ding, *Eur. Polym. J.*, 2005, **41**, 2161; (*b*) X. Y. Xiong, K. C. Tama and L. H. Gan, *Polymer*, 2005, **46**, 1841.

21 (*a*) M. T. Rodrigues, R. L. Reis and M. E. Gomes, *J. Tissue Eng. Regen. Med.*, 2013, **9**, 673; (*b*) G. Vunjak-Novakovic, G. Altman, R. Horan and D. L. Kaplan, *Annu. Rev. Biomed. Eng.*, 2004, **6**, 131.

22 C. Kuo, J. Marturano and R. Tuan, *Sports Med. Arthrosc. Rehab. Ther. Technol.*, 2010, **2**, 20.

23 J. E. Moreau, D. S. Bramono, R. L. Horan, D. L. Kaplan and G. H. Altman, *Tissue Eng., Part A*, 2008, **14**, 1161.

24 J. Z. Paxton, L. M. Grover and K. Baar, *Tissue Eng., Part A*, 2010, **16**, 3515.

25 E. W. Yates, A. Rupani, G. T. Foley, W. S. Khan, S. Cartmell and S. J. Anand, *Stem Cells Int.*, 2012, **2012**, 438125.

26 E. M. Raïf, B. B. Seedhom, M. J. Pullan and T. Toyoda, *Tissue Eng.*, 2007, **13**, 629.

27 (*a*) A. Hoffmann, G. Pelled, G. Turgeman, P. Eberle, Y. Zilberman, H. Shinar, K. Keinan-Adamsky, A. Winkel, S. Shahab, G. Navon, G. Gross and D. Gazit, *J. Clin. Invest.*, 2006, **116**, 940; (*b*) C. A. Gregory, J. Ylostalo and D. J. Prockop, *Sci. STKE*, 2005, **294**, 37; (*c*) B. Neuhuber, S. A. Swanger, L. Howard, A. Mackay and I. Fischer, *Exp. Hematol.*, 2008, **36**, 1176.

28 (*a*) A. Kowalski, A. Duda and S. Penczek, *Macromolecules*, 1998, **31**, 2114; (*b*) M.-H. Huang, S. Li and M. Vert, *Polymer*, 2004, **45**, 8675.

29 A. C. Vieira, R. M. Guedes and A. T. Marques, *J. Biomech.*, 2009, **42**, 2421.

30 L. Fambri, A. Pegoretti, R. Fenner, S. D. Incardona and C. Migliaresi, *Polymer*, 1997, **38**, 79.

31 J. W. Freeman, M. D. Woods and C. T. Laurencin, *J. Biomech.*, 2007, **40**, 2029.

32 (*a*) H. H. Jung, K. Park and D. K. Han, *J. Controlled Release*, 2010, **147**, 84; (*b*) A. Rey-Rico, M. Silva, J. Couceiro, A. Concheiro and C. Alvarez-Lorenzo, *Eur. Cell. Mater.*, 2011, **21**, 317.

33 (*a*) J. E. Moreau, J. Chen, R. L. Horan, D. L. Kaplan and G. H. Altman, *Tissue Eng.*, 2005, **11**, 1887; (*b*) J. Chen, R. L. Horan, D. Bramono, J. E. Moreau, Y. Wang, L. R. Geuss, A. L. Collette, V. Volloch and G. H. Altman, *Tissue Eng.*, 2006, **12**, 3085.

34 (*a*) R. Schweitzer, J. H. Chyung, L. C. Murtaugh, A. E. Brent, V. Rosen, E. N. Olson, A. Lassar and C. J. Tabin, *Development*, 2001, **128**, 3855; (*b*) P. Cserjesi, D. Brown, K. L. Ligon, G. E. Lyons, N. G. Copeland, D. J. Gilbert, N. A. Jenkins and E. N. Olson, *Development*, 1995, **121**, 1099.

35 (*a*) C. Shukunami, A. Takimoto, M. Oro and Y. Hiraki, *Dev. Biol.*, 2006, **298**, 234; (*b*) D. Docheva, E. B. Hunziker, R. Fässler and O. Brandau, *Mol. Cell. Biol.*, 2005, **25**, 699.

36 (*a*) A. Hoffmann, G. Pelled, G. Turgeman, P. Eberle, Y. Zilberman, H. Shinar, K. Keinan-Adamsky, A. Winkel, S. Shahab, G. Navon, G. Gross and D. Gazit, *J. Clin. Invest.*, 2006, **116**, 940; (*b*) D. Noël, D. Gazit, C. Bouquet, F. Apparailly, C. Bony, P. Plence, V. Millet, G. Turgeman, M. Perricaudet, J. Sany and C. Jorgensen, *Stem Cells*, 2004, **22**, 74; (*c*) J. M. Li, Y. Zhang, Y. Ren, B. G. Liu, X. Lin, J. Yang, H. C. Zhao, Y. J. Wang and L. Song, *PLoS One*, 2014, **9**, e106598.